Electronic Absorption Spectra of $H_2C_6O^+$ Isomers: Produced by Ion-Molecule Reactions

Journal:	*The Journal of Physical Chemistry*
Manuscript ID:	jp-2014-09561v.R1
Manuscript Type:	Article
Date Submitted by the Author:	11-Dec-2014
Complete List of Authors:	Chakraborty, Arghya; University of Basel, Department of Chemistry Fulara, Jan; University of Basel, Department of Chemistry Maier, John; University of Basel, Department of Chemistry

Electronic Absorption Spectra of $H_2C_6O^+$ Isomers: Produced by Ion-Molecule Reactions

Arghya Chakraborty, Jan Fulara and John P. Maier*
Department of Chemistry, University of Basel, Klingelbergstrasse 80, CH-4056, Basel, Switzerland

Abstract

Three absorption systems with origin at 354, 497 and 528 nm were detected after mass-selected deposition of $H_2C_6O^+$ in a 6 K neon matrix. The ions were formed by the reaction of C_2O with HC_4H^+ in a mixture of C_3O_2 and diacetylene in a hot cathode source, or by dissociative ionization of tetrabromocyclohexadienone. The 497 and 354 nm systems are assigned to the **1** ^{2}A" ← X ^{2}A" and **2** ^{2}A" ← X ^{2}A" electronic transition of $\mathbf{B}^+$, (2-ethynylcycloallyl)methanone cation and the 528 nm absorption to **1** $^2A_2$ ← X $^2B_1$ of $\mathbf{F}^+$, 2-ethynylbut-3-yn-1-enone-1-ylide, on the basis of calculated excitation energies with CASPT2.

Keywords: electronic spectra, mass-selection, $H_2C_6O^+$, neon matrices, oxygenated hydrocarbons.

*Corresponding Author: J. P. Maier, Tel. +41 612673826, Fax. +41 612673855
Email address: j.p.maier@unibas.ch

1. Introduction

Production of oxygenated hydrocarbons in interstellar clouds is a challenging issue in astrochemical research. Though oxygen has a cosmic abundance similar to carbon, the number of oxo-organic species detected in interstellar and protostellar regions is smaller than hydrocarbons.[1-4] A reason is that oxygen is locked up in the oxides of carbon, silicon and refractory metals, and CO is the most abundant molecule, after H_2, in space.[5-10]

One of the ways to produce oxygen containing species in the interstellar medium (ISM) is radiative association of atomic oxygen with hydrocarbons.[2] An example of this could be cyclopropenone c-H_2C_3O which has been detected in Sagittarious B2(N),[11] a region where cyclopropenylidene c-C_3H_2 has also been observed. Recently, the larger abundance of long chain hydrocarbon anions in denser clouds has been attributed to the depletion of oxygen atoms. Postulated reaction models suggest that these anions react with oxygen atoms and form oxygenated hydrocarbon and carbon oxides.[12] Carbon monoxide is also taken into account for the formation of oxygenated species in the ISM via radiative association reactions.[13]

In this context, reactions of some astrochemically relevant ions as C_4H^+, $C_4H_2^+$, $C_4H_3^+$, C_5H^+, C_6H^+ with CO and O_2 were studied by the selected-ion flow tube technique. All of these species reacted with CO giving mono-oxygenated hydrocarbon cations.[13] HCO^+, HCO_2^+, H_3CO^+ are the only three oxygen containing hydrocarbon cations detected so far in the ISM by radioastronomy.[14-17] In the laboratory several mono-oxygenated hydrocarbons HC_nO n = 1 – 7 were studied by microwave spectroscopy.[18-22] Few oxides of carbon chains are studied in rare gas matrices as well [23,24] but spectroscopy of oxygenated hydrocarbon cations is unknown.

In this contribution the electronic absorption spectra of $H_2C_6O^+$ trapped in 6 K neon matrices are presented and assigned to two isomers on the basis of calculated excitation energies

using the CASPT2 method. These mono-oxygenated hydrocarbon cations are formed *via* a reaction of C_2O with hydrocarbon cations in the discharge source.

2. Experimental

2.1 Production of Ions

A 1:1 mixture of carbon suboxide and diacetylene diluted with helium was used to produce $H_2C_6O^+$ in a hot discharge source. Pure C_3O_2 or HC_4H does not yield the *m/z*=90 peak in the mass spectrum but it appears in their mixture (Figure 1, green trace). The C_2O^+ and CO^+ fragment ions are present in the mass spectrum of C_3O_2 (Figure 1, red) and in the mixture with HC_4H. $H_2C_6O^+$ can be formed in the source by insertion of the C_2O^+ fragment into HC_4H, or C_2O into HC_4H^+. As HC_6H^+ is present in the mass spectrum of diacetylene, as well as in the mixture with carbon suboxide, formation of $H_2C_6O^+$ could also proceed *via* reaction of CO/CO^+ with HC_6H^+/HC_6H. However, this is excluded because the *m/z*=90 cation was not observed with a CO/HC_4H mixture under similar condition whereas the mass peak of HC_6H^+ was intense. It was found that the intensity of the C_2O^+ and $H_2C_6O^+$ ions produced under different discharge conditions are correlated, suggesting that the formation of $H_2C_6O^+$ depends on the production of C_2O^+. $H_2C_6O^+$ was also produced from a vapor of 2, 4, 4, 6-tetrabromo-2,5-cyclohexadienone (TBrC).

2.2 Matrix Isolation Spectroscopy

The method used combines mass-selection with matrix isolation spectroscopy.[25] Ions produced in the source are extracted by electrostatic lenses and then deflected 90° to eliminate neutrals. The *m/z*=90 cations are selected in a quadruple mass filter and subsequently co-deposited with neon (containing trace of chloromethane in a ratio 1:20000) on a sapphire plate coated with rhodium held at 6 K. CH_3Cl captures free electrons emitted from metal surfaces by impact of ions, diminishing the neutralization of cations and reducing the space charge. CH_3Cl breaks into $CH_3^{\bullet}$ and Cl^- by dissociative electron attachment, but these species do not interfere with the

absorption measurements in the visible and ultraviolet regions. Ions were also deposited in neon without CH_3Cl to obtain a higher concentration of neutrals. The growth of the matrix to 100-150 μm thickness is controlled by observing light transmittance.

Spectra were recorded in the 250-1100 nm range by 60 nm overlapping sections. Halogen and high pressure xenon arc lamps were used as sources and light after travelling through the 20 mm length of matrix was collected by optical fibers and transferred to the entrance slit of the spectrograph, wavelength dispersed and recorded by the CCD cameras.

3. Computation

Several structures (shown in chart 1) can be expected for $H_2C_6O^+$ formed *via* ion – molecule reactions between C_2O and HC_4H^+, C_2O^+ / HC_4H or fragmentation of TBrC. The ground state geometries of nine plausible structures ($\mathbf{A}^+$ - $\mathbf{I}^+$) were optimized using the MP2 method with the cc-pVTZ basis set with the Gaussian 09 program.[26] The ground state vibrations were calculated for each molecule to find real minima. The most stable is isomer $\mathbf{A}^+$; $\mathbf{B}^+$, $\mathbf{C}^+$, $\mathbf{D}^+$, $\mathbf{E}^+$ and $\mathbf{F}^+$ lie 40 - 60 kJ/mol and $\mathbf{G}^+$, $\mathbf{H}^+$, $\mathbf{I}^+$ 140 - 265 kJ/mol to higher energy. Among the neutral counterparts structure **C** is the global minimum and **D** is less stable by 8 kJ/mol.

The equilibrium coordinates obtained from the MP2 method were refined with the second order multi-configurational perturbation theory (CASPT2) implemented in the Molcas software.[27,28] The CASPT2 calculations to obtain the ground - state geometries of the $H_2C_6O^+$ isomers were carried with the 9 / 9 active space. These coordinates were used for the prediction of vertical electronic excitation energies. The calculations with a larger active space (11 / 11) used the multi – state (MS) CASPT2 option, with wave functions optimized for the average energy of eight roots. Vertical excitation energies of **B** and **F** were also obtained at the MS-CASPT2 level with a 12 / 12 active space.

4. Results and Discussion

Moderately intense absorptions are detected in the 320─530 nm region (Figure 2, upper traces) after trapping in neon mass selected $H_2C_6O^+$ produced from a 1:1 mixture of C_3O_2 and diacetylene. Two groups of bands, which differ in width, are apparent in the spectrum. The narrower features start around 528, 362 and 329 nm and broader ones at ~ 497 and ~ 354 nm. The 362 and 329 nm absorptions are **2** $^2\Pi_g \leftarrow X\ ^2\Pi_u$ and **3** $^2\Pi_g \leftarrow X\ ^2\Pi_u$ transitions of *l*-HC_5H^+.[29] These have been measured in an earlier study and are shown in the red trace of Figure 3 with the absorptions detected after deposition of $H_2C_6O^+$ in black. The traces were scaled to the intensity of the 362 nm band. The HC_5H^+ cation is produced in the matrix as a result of collisionally induced fragmentation of $H_2C_6O^+$ during deposition.

The matrix was exposed for 20 min to UV light ($\lambda > 260$) nm resulting in the detachment of electrons from Cl^- and neutralization of cations. The spectrum obtained is shown as the lower traces Figure 2. The absorptions starting at 528, 497 and 354 nm almost disappeared whereas the ones of HC_5H^+ reduced. The HC_5H^+ bands behave in a regular way under UV irradiation – their intensity decreases because of neutralization – whereas for the new absorptions additional decay channels are open: isomerization or/and fragmentation. No new peaks appeared after UV irradiation. $H_2C_6O^+$ ions were also deposited in a pure neon matrix but only a weak absorption at 528 nm was detected. Deposition of ions without the CH_3Cl scavenger favors trapping of neutral counterparts because of electron availability in the matrix. The behavior of the absorption features in Figure 2 under exposure to UV light indicates that they belong to photo - unstable isomer/s of $H_2C_6O^+$. Because the neutral counterparts of $H_2C_6O^+$ were not observed after photobleaching, or in pure neon, they do not have electronic transitions in the 250-1100 nm detection range, or these are weak.

The excitation energies of the neutral counterparts of the observed cations were calculated with MS-CASPT2 to explain why their absorptions were not observed. The results are

collected in Table SI1 (SI =Supporting Information). As can be seen the strongest transitions fall in the UV range beyond the experimental detection range.

$H_2C_6O^+$ was also produced from TBrC and deposited. The spectrum obtained consists of two broader features starting at 497 and 354 nm and a weak absorption at 528 nm (Figure 4, red trace). After irradiation (260─390 nm) the 497 and 354 nm absorptions diminish substantially, implying that they belong to the same $H_2C_6O^+$ isomer. The decay of the absorptions under such irradiation conditions is due to photo – instability of the cation, because neutralization is not efficient at these wavelengths.

Use of different precursors for the production of $H_2C_6O^+$ established that two isomers contribute to the spectra (Figures 2 – 4). One has a weak transition in the visible (2.49 eV; 497 nm) and a much stronger in the UV (3.51 eV; 354 nm). The second cation is characterized by the strong transition in the visible (2.35 eV; 528 nm) with resolved vibrational structure.

Vertical excitation energies of nine $H_2C_6O^+$ isomers were calculated with MS-CASPT2 to assign the observed absorptions to specific species. The results for the likely candidates are collected in Table 1 and for the remaining ones in Table SI2. Among these only structures $\mathbf{B}^+$ and $\mathbf{D}^+$ can be responsible for the two absorptions at 497 and 354 nm. The calculations predict a moderately intense transition with energy 2.68 (f =0.024) and 2.60 eV (f=0.040) and about a ten times stronger transition at 3.68 and 3.67 eV for $\mathbf{B}^+$ and $\mathbf{D}^+$, respectively. The oscillator strengths are in accord with the intensities of the 497 and 354 nm systems. The vertical excitation energies overestimate the onsets of the observed systems by ~ 0.2 eV; calculated adiabatic values should match better with the experimental ones. As $\mathbf{D}^+$ lies only slightly higher in energy than $\mathbf{B}^+$, it can not be eliminated from consideration as the carrier.

In contrast to isomers $\mathbf{B}^+$ and $\mathbf{D}^+$, for which the spectroscopic signature are the two electronic systems in the visible and UV, the carrier of the 528 nm system should possess only a single strong transition around 2.35 eV. Apart from isomers $\mathbf{B}^+$ and $\mathbf{D}^+$ four others: $\mathbf{C}^+$, $\mathbf{E}^+$, $\mathbf{F}^+$ and $\mathbf{G}^+$ have transitions in this region. The first electronic system of $\mathbf{E}^+$ at 2.45 eV is weak

(f = 0.006) and two stronger ones (f = 0.02 and 0.065) are predicted in the 3.1 - 3.3 eV range, in contrast to the observation. The first electronic transition of $\mathbf{G}^+$ is calculated at 2.26 eV with f = 0.085, the next one at 3.22 eV (f = 0.045), but it can be excluded as the carrier because its UV transition should also be detectable. Isomer $\mathbf{C}^+$ is also eliminated from consideration: although the **1** ^{2}A" ← X ^{2}A" electronic transition at 2.51 eV is very strong (f = 0.2), an equally intense band at 3.92 eV is predicted, in contrast to the observation.

Isomer $\mathbf{F}^+$ fulfils the criteria for the carrier of 528 nm system: a strong transition at 2.38 eV (f=0.11) close to the observation (2.35 eV) and a non-detectable absorption in the UV. The next strongest transition of $\mathbf{F}^+$ is predicted at 5.58 eV (f=0.055), beyond the experimental detection range. Moreover, $\mathbf{F}^+$ during depositing with ~50 eV kinetic energy on solid neon can fragment to produce *l*-HC_5H^+ and CO. The absorptions of *l*-HC_5H^+ are detected (Figure 2). Therefore the 528 nm system is assigned to the **1** $^2A_2$ ← X $^2B_1$ transition of $\mathbf{F}^+$. A well resolved vibrational structure is apparent in the spectrum and results from the excitation of the ν_7, ν_6 and ν_3 vibrational modes and their combinations. The assignment is based on the harmonic frequencies calculated for the ground state of $\mathbf{F}^+$ with the DFT method using the B3LYP functional and cc-pVTZ basis set (see Table 2).

The reactants which lead to the formation of $H_2C_6O^+$ are C_2O and HC_4H^+, and/or C_2O^+ with HC_4H, as both cations were observed in the mass spectrum of the precursor. The ionization potential (IP) of diacetylene is 10.17 eV,[30] but the experimental value for C_2O is unknown. Therefore the IPs of HC_4H and C_2O were calculated using the CCSD(T) method for the geometry optimized at the CCSD level leading to 10.08 eV for HC_4H and 10.81 eV for C_2O. Hence, the most probable way of $H_2C_6O^+$ production is the reaction of C_2O with HC_4H^+. The reactions of C_2O^+ with diacetylene, as well as C_2O with HC_4H^+, are exothermic. The calculated enthalpy of the reaction between C_2O with HC_4H^+ is 539 kJ/mol at the MP2/cc-pVTZ level of theory. C_2O in the $^3\Sigma^-$ ground state is a reactive biradical with two electrons on the terminal -

carbon atom. C_2O attacks the electrophilic center of HC_4H^+ which is located on the middle carbon atoms (Table SI3).

In the case of the reaction C_2O^+ with HC_4H, a charge - exchange is likely the first step. C_2O^+ in the $^2\Pi$ ground state possesses an unpaired electron on the terminal carbon atom and reacts as a radical. The preferred site of reaction of C_2O^+ with diacetylene is on the electronegative carbon atom adjacent to the hydrogen atoms (Table SI3).

On the basis of the calculated vertical excitation energies and the oscillator strengths (Table 1) as well as the ground state stabilities (Chart 1) of $\mathbf{B}^+$ and $\mathbf{D}^+$, one cannot firmly deduce the carrier for the 497 and 354 nm absorptions. However, the structure of $\mathbf{B}^+$ produced *via* dissociative ionization of TBrC is analogous to that of the $C_6H_4^+$ isomer: three carbon – member ring with aliphatic chain ($\mathbf{T}^+$) generated from 1,2-dibromobenzene under similar discharge condition.[31] MS-CASPT2 calculation predicts strong electronic transition (f=0.2) at 4.45 eV (280 nm) for neutral **D** which was not observed (See Table SI1). Thus, the 497 and 354 nm systems are assigned to the **1** ^{2}A" ← X ^{2}A" and **2** ^{2}A" ← X ^{2}A" electronic transitions of $\mathbf{B}^+$.

5. Conclusions

Two isomers of $H_2C_6O^+$ (2-ethynylcycloallyl)methanone cation $\mathbf{B}^+$ and 2-ethynylbut-3-yn-1-enone-1-ylide, $\mathbf{F}^+$ were produced in a hot cathode discharge source from a mixture of carbon suboxide and diacetylene. The reactions between C_2O and HC_4H^+, or C_2O^+ and HC_4H, are exothermic. They should be considered in the astrophysical models as a way of incorporation of oxygen into the hydrocarbon moieties. Three absorption systems starting at 528, 497 and 354 nm are detected following deposition of $H_2C_6O^+$ in a 6 K neon matrix. These are assigned to the **1** $^2A_2$ ← X $^2B_1$ electronic transition of $\mathbf{F}^+$, and **1** ^{2}A" ← X ^{2}A" and **2** ^{2}A" ← X ^{2}A" of $\mathbf{B}^+$, on the basis of mass-selection, the cationic nature and the calculated excitation energies with the CASPT2 method. The $\mathbf{B}^+$ and $\mathbf{F}^+$ isomers were found unstable under 260─390 nm photon

exposure. Oxygenated hydrocarbons and their ions, such as $H_2C_6O^+$, are likely reactive intermediates in combustion, and the present spectroscopic data provide the means to monitor them in situ via their electronic absorptions and can serve as starting point for the gas phase study.

Acknowledgement: This work was supported by the Swiss National Science Foundation (project 200020-124349/1).

Supporting Information

Tables contain calculated excitation energies of five cation and three neutral isomers and also Mulliken charges and spin densities of HC_4H/ HC_4H^+ and C_2O/C_2O^+. This material is available free of charge via the Internet at http://pubs.acs.org.

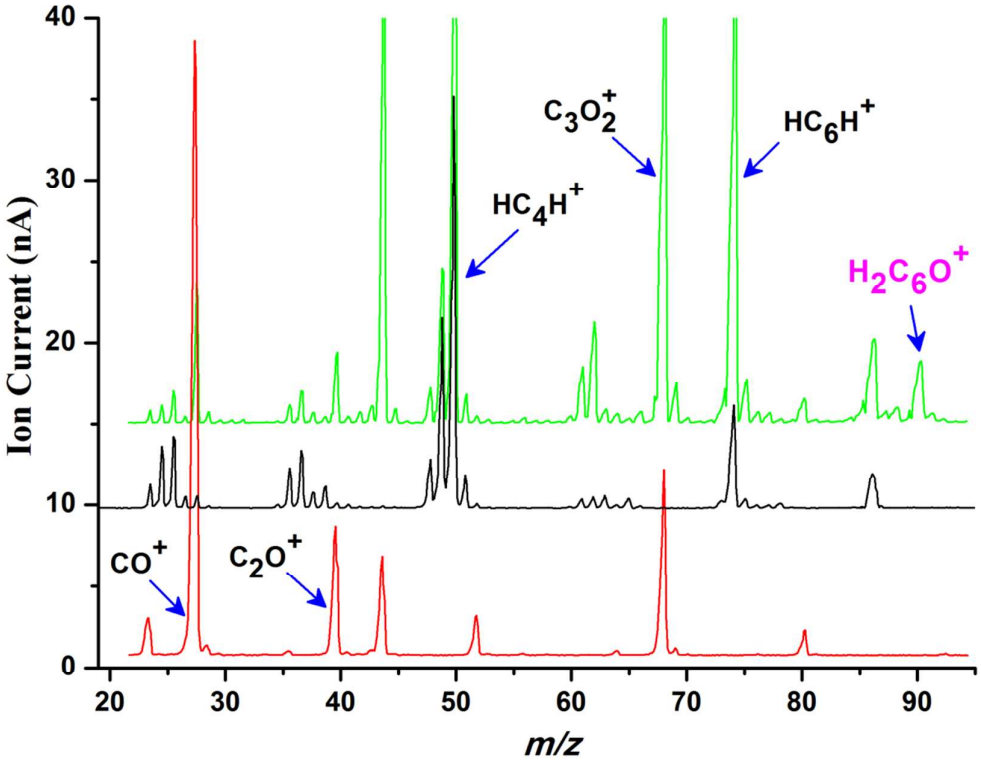

Figure 1. Mass spectra of C_3O_2 (red), HC_4H (black) and 1:1 mixture of C_3O_2 and HC_4H (green). The $H_2C_6O^+$ (m/z = 90) peak appeared upon mixing C_3O_2 and HC_4H.

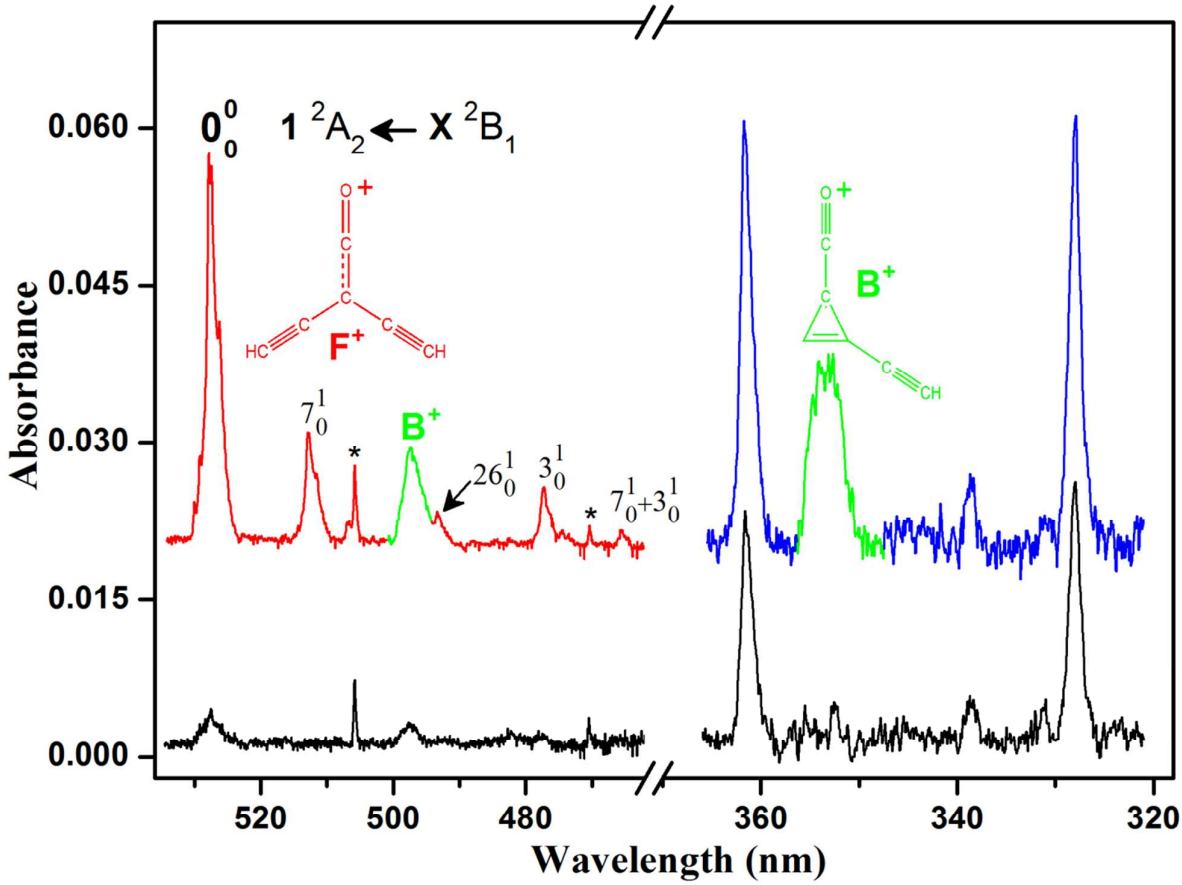

Figure 2. Electronic absorption spectra recorded after deposition of $H_2C_6O^+$ produced from a 1:1 mixture of C_3O_2 and diacetylene (upper traces) and after 20 minute irradiation with λ>260 nm photons (lower traces). Bands denoted by * belong to C_2^+.

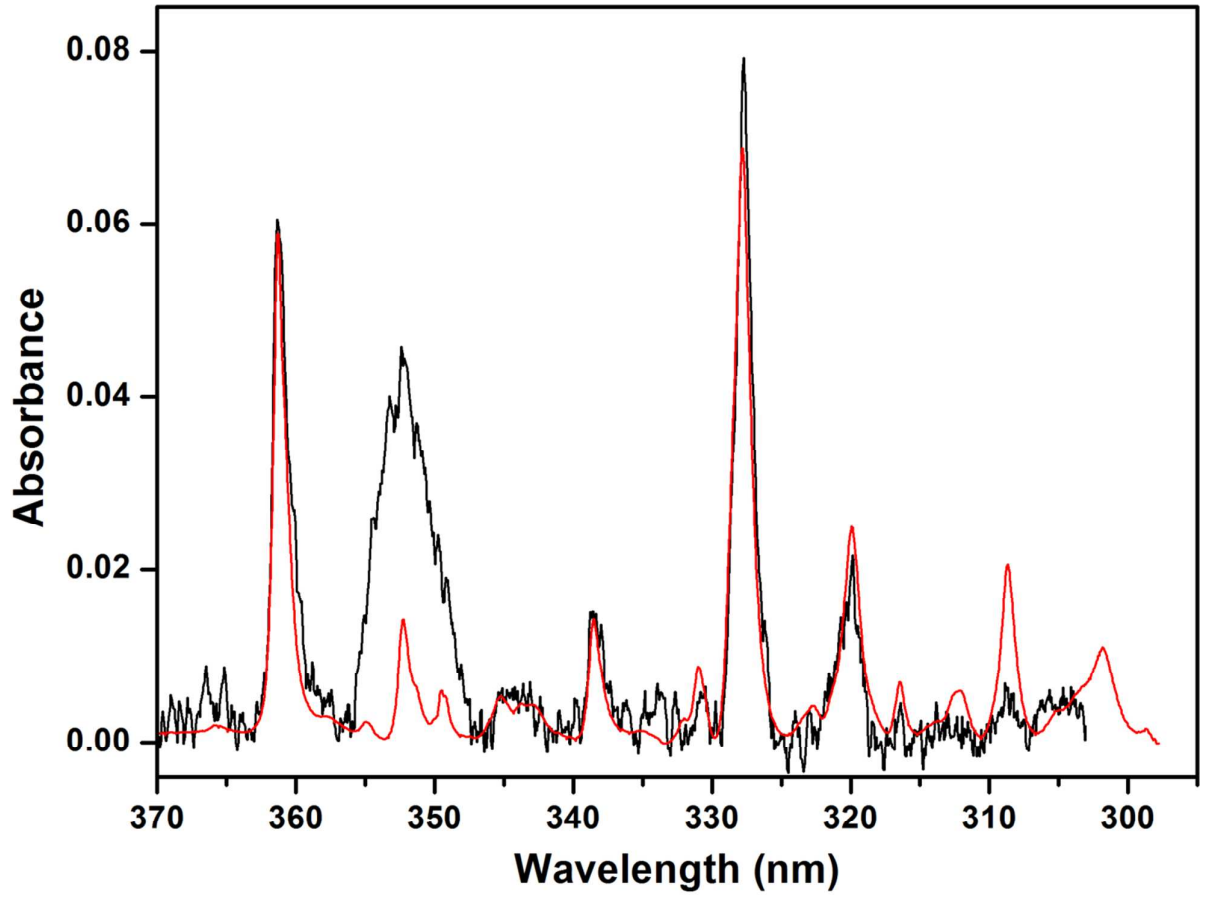

Figure 3. Electronic absorption spectra recorded after deposition of $H_2C_6O^+$ generated from a 1:1 mixture of C_3O_2 and diacetylene (black), and after deposition of HC_5H^+ produced from diacetylene (red). The spectrum of HC_5H^+ is normalized to the intensity of the 362 nm band.

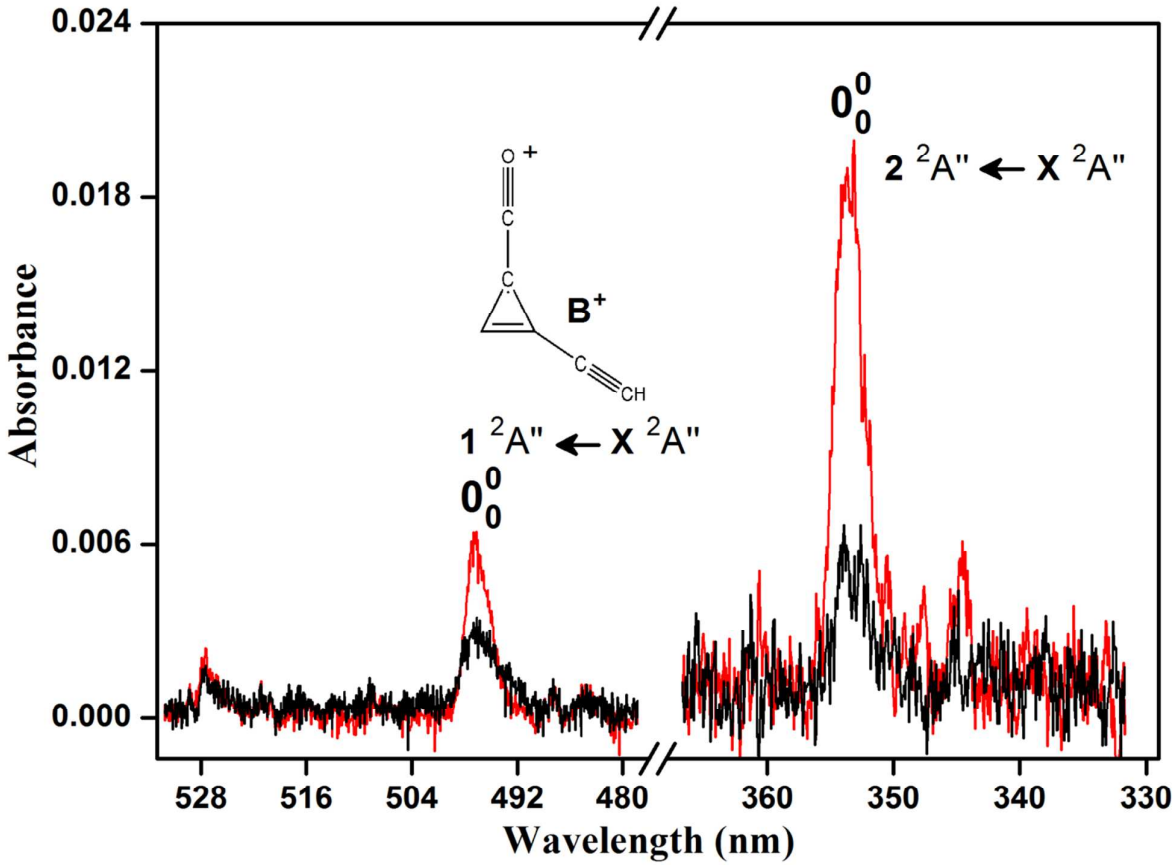

Figure 4. Electronic absorption spectrum of $H_2C_6O^+$ obtained after deposition of *m/z* = 90 ions produced from 2, 4, 4, 6-tetrabromo-2,5-cyclohexadienone (TBrC) – red, and after 20 min. irradiation with 250 - 390 nm photons – black.

Chart 1. Structures and relative ground state energies (kJ mol^{-1}) of H_2C_6O cations (**bold**) and neutrals (*italic*), calculated with the MP2 method and cc-pVTZ basis set. Bond lengths (Å) correspond to the optimized cation geometries.

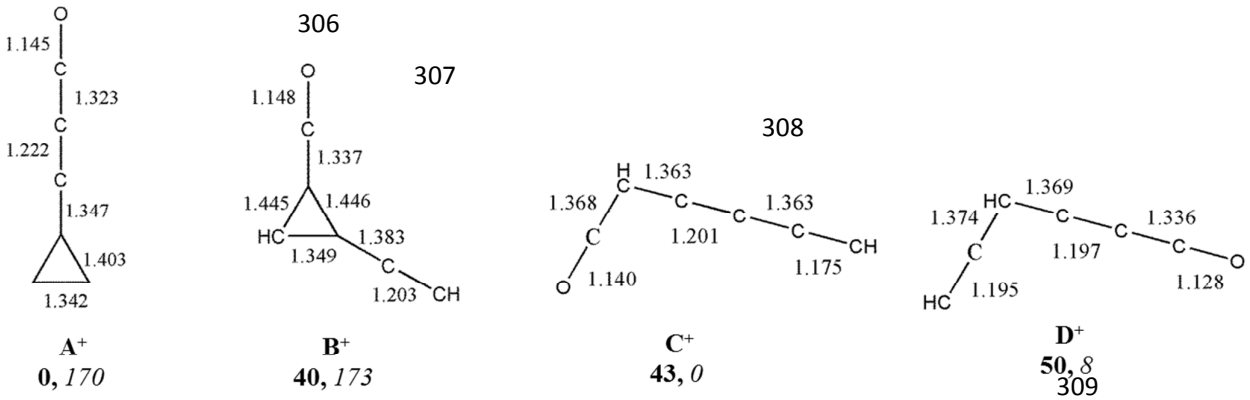

A$^+$ **0,** *170* **B**$^+$ **40,** *173* **C**$^+$ **43,** *0* **D**$^+$ **50,** *8*

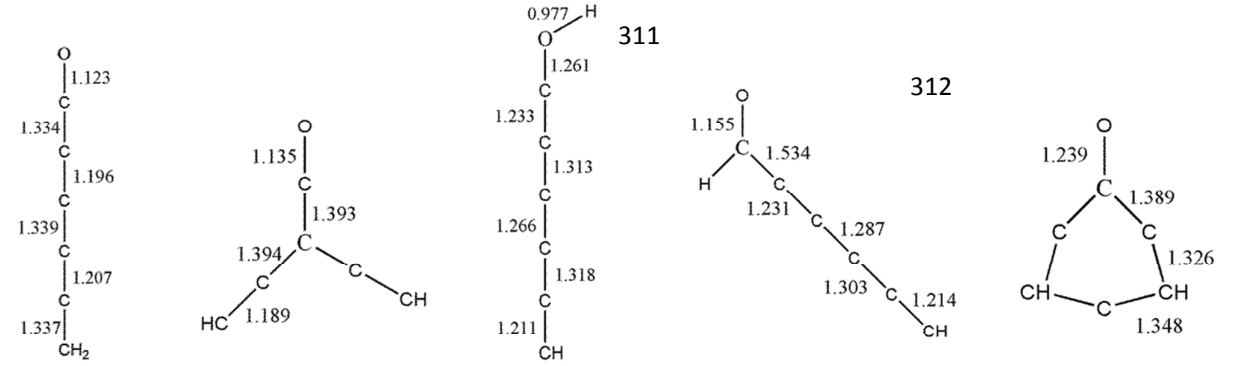

E$^+$ **58,** *44* **F**$^+$ **60,** *37* **G**$^+$ **147,** *109* **H**$^+$ **257,** *281* **I**$^+$ **265,** *192*

Table 1. Excitation energies E_{cal} (eV) and oscillator strengths (f) of $H_2C_6O^+$ isomers calculated by the MS-CASPT2 method and comparison with the observations (E_{obs}).

Species	Transitions	E_{cal}	f	E_{obs}
B$^+$ (C_S)	**1** $^2A''$ ← X $^2A''$	**2.68**	0.024	2.49
	2 $^2A''$ ←	**3.68**	0.200	3.51
	3 $^2A''$ ←	5.32	0.100	
	4 $^2A''$ ←	5.73	0.060	
D$^+$ (C_S)	**1** $^2A''$ ← X $^2A''$	2.60	0.040	
	2 $^2A''$ ←	3.67	0.49	
	3 $^2A''$ ←	4.16	0.0069	
	4 $^2A''$ ←	4.44	0.0044	
	5 $^2A''$ ←	4.70	0.015	
F$^+$ (C_{2V})	**1** $^2A_2$ ← X $^2B_1$	**2.38**	0.11	2.35
	2 $^2A_2$ ←	5.58	0.051	
	1 $^2B_1$ ←	4.26	0.007	
	2 $^2B_1$ ←	5.30	0.27	
	2 $^2B_1$ ←	5.90	0.005	
C$^+$ (C_S)	**1** $^2A''$ ← X $^2A''$	2.51	0.19	
	2 $^2A''$ ←	3.92	0.17	
	3 $^2A''$ ←	4.08	0.030	
	4 $^2A''$ ←	4.47	0.15	

Table 2.Absorption band maxima (±0.1nm) of electronic transitions of $H_2C_6O^+$ isomers $\mathbf{B}^+$ and $\mathbf{F}^+$ in 6 K neon matrices and assignment based on MS-CASPT2 calculations. The vibrational interpretation of the $\mathbf{F}^+$ spectrum is based on the calculated ground – state harmonic frequencies (footnote).

Species	λ (nm)	ν (cm^{-1})	Δν (cm^{-1})	Assignment	
$\mathbf{F}^+$	527.6	18954	0	0_0^0	$\mathbf{1}\ ^2B_1 \leftarrow \mathbf{X}\ ^2A_2$
	512.8	19501	547	ν_7	
	493.1	20280	1326	$2\nu_6$	
	476.9	20969	2015	ν_3	
	465.0	21505	2551	$\nu_3 + \nu_7$	
$\mathbf{B}^+$	497.3	20109	0	0_0^0	$\mathbf{1}\ ^2A'' \leftarrow \mathbf{X}\ ^2A''$
	353.6	28281	0	0_0^0	$\mathbf{2}\ ^2A'' \leftarrow \mathbf{X}\ ^2A''$

Totally-symmetric vibrations (cm^{-1}) of $\mathbf{F}^+$ calculated with DFT using the B3LYP functional and the cc-pVTZ basis set: ν_1 to ν_7; 3412, 2276, 2169, 1198, 754, 669, 543, 121.

References:

1) Cameron, A. G. W. Abundances of the Elements in the Solar System. *Space Sci. Rev.* **1973**, *15*, 121-146.

2) Snow, T. P.; Bierbaum, V. M. Ion Chemistry in the Interstellar Medium. *Annu. Rev. Anal. Chem.* **2008**. *1*, 229–259.

3) Thaddeus, P.; McCarthy, M.C. Carbon Chains and Rings in the Laboratory and in Space. *Spectrochimica Acta Part A.* **2001**, *57* , 757–774.

4) Lee, J-E.; Evans, N. J.; Shirley, Y. L. Chemistry and Dynamics in Pre-Protostellar Cores. *Astrophys. J.* **2013**, *583*,789-808.

5) Solomon, P.; Jefferts, K. B.; Penzias, A. A.; Wilson, R. W. Observation of CO Emission at 2.6 Millimeters from IRC+10216. *Astrophys. J.* **1971**, *163*, L53-L56.

6) Smith, A. M.; Stecher, T.P. Carbon Monoxide in the Interstellar Spectrum of Zeta Ophiuchi. *Astrophys. J.* **1971**, *164*, L43-L47.

7) Dickinson, D. F. Detection of Silicon Monoxide at 87 GHz. *Astrophys. J.* **1972**, *175*, L43-L46.

8) Tenenbaum, E. D.; Woolf, N. J.; Ziurys, L. M. Identification of Phosphorus Monoxide ($X\,^2\Pi_r$) in VY Canis Majoris: Detection of the First P–O Bond in Space. *Astron.Astrophys.* **2007**, *666*, L29–L32.

9) Tenenbaum, E. D.; Ziurys, L. M. Millimeter Detection of AlO ($X\,^2\Sigma^+$): Metal Oxide Chemistry in the Envelope of VY Canis Majoris. *Astrophys. J.* **2009**, *694*, L59–L63.

10) Hillenbrand, L. A.; Knapp, G. R.; Padgett, D. L.; Rebull, L. M.; McGehee, P. M. Optical TiO and VO Band Emission in Two Embedded Protostars: IRAS 04369+2539 and IRAS 05451+0037. *Astron. J.* **2012**, *143,* 1-13.

11) Hollis, J. M.; Remijan, A. J.; Jewell, P. R.; Lovas, F. J. Cyclopropenone (c-H_2C_3O): A New Interstellar Ring Molecule. *Astrophys. J.* **2006**, *642*, 933-939.

12) Cordiner, M. A.; Charnley, S. B. Gas-Grain Models for Interstellar Anion Chemistry. *Astrophys. J.* **2012**, *749*, 120(1-10).

13) Adams, N. G.; Smith, D.; Giles, K.; Herbst, E. The Production of C_nO, HC_nO and H_2C_nO Molecules in Dense Interstellar Clouds. *Astron. Astrophys.* **1989**, *220*, 269-271.

14) Klemperer, W. Carrier of the Interstellar 89.190 GHz Line. *Nature.* **1970**, *227*, 1230.

15) Thaddeus, P.; Guelin, M.; Linke, R. A. Three New 'Nonterrestrial' Molecules. *Astrophys. J.* **1981**, *246*, L41–L45.

16) Mihn, Y. C.; Irvine, W. M.; Ziurys, L. M. Observations of Interstellar $HOCO^+$ – Abundance Enhancements toward the Galactic Center. *Astrophys. J.* **1988**, *334*, 175–181.

17) Ohishi, M.; Ishikawa, S-I.; Amano,T.; Oka, H.; Irvine, W. M.; Dickens, J. E.; Ziurys, L. M.; Apponi, A. J. Detection of A New Interstellar Molecular Ion, H_2COH^+ (Protonated Formaldehyde). *Astrophys. J.* **1996**, *471*, L61–L64.

18) Blake, G. A.; Sastry, K. V. L. N.; De Lucia, F. C. The Laboratory Millimeter and Submillimeter Spectrum of of HCO. *J. Chem. Phys.* **1984**, *80* , 95-101.

19) Endo, Y.; Hirota, E. The Submillimeter-Wave Spectrum of the HCCO Radical. *J. Chem. Phys.* **1987**, *86*, 4319 -4326.

20) Cooksy, A. L.; Watson, J. K. G.; Gottlieb, C. A.; Thaddeus, P. The Structure of the HCCCO Radical. Rotational Spectra and Hyperfine Structure of Monosubstituted Isotopomers. *J. Chem. Phys.* **1994**, *101*,178-186.

21) Kohguchi, H.; Ohshima, Y.; Endo, Y. Pulsed-Discharge Nozzle Fourier-Transform Microwave Spectroscopy of the HC_4O Radical. *J. Chem. Phys*. **1994**, *101*, 6463-6469.

22) Mohamed, S.; McCarthy, M. C.; Cooksy, A. L.; Hinton, C.; Thaddeus, P. Rotational Spectra of the Carbon-Chain Radicals HC_5O , HC_6O and HC_7O. *J. Chem. Phys.* **2005**, *123*, 234301 (1-8).

23) Strelnikov, D.; Reusch, R.; Krätschmer, W. Oxides of Long Carbon Chains: Results Obtained on IR and UV–Vis Absorptions. *J. Mol. Spec.* **2007**, *243*, 189-193.

24) Joseph, S. M. E.; Fulara, J.; Garkusha, I.; Maier, J. P. Electronic Absorption Spectra of C_7O and C_7O^+ in 6 K Neon Matrices. *Mol. Phys.* **2013**, *111*, 1977-1982.

25) Nagy, A.; Garkusha, I.; Fulara. J.; Maier, J. P. Electronic Spectroscopy of Transient Species in Solid Neon: The Indene Motif Polycyclic Hydrocarbon Cation Family $C_9H_y^+$ (y=7-9) and their Neutrals. *Phys. Chem. Chem. Phys*. **2013**, *15*, 19091-19101.

26) Frisch, M. J.; Trucks, G. W.; Schlegel, H. B.; Scuseria, G. E.; Robb, M. A.; Cheeseman, J. R.; Scalmani, G.; Barone, V.; Mennucci, B.; Petersson, G. A.; et al. Gaussian 09, revision D.01; Gaussian, Inc.:Wallingford, CT, **2009.**

27) Andesson, K.; Malmqvist,P.-A.; Roos, B. O.; Sadlej, A. J. Wolinski, K. Second-Order Perturbation Theory with a CASSCF Reference Function. *J. Phys. Chem*. **1990**, *94*, 5483-5488.

28) Andesson, K.; Malmqvist, P.-A.; Roos, B. O. Second-Order Perturbation Theory with a Complete Active Space Self-Consistent Field Reference Function. *J. Chem. Phys*. **1992**, *96*, 1218-1226.

29) Fulara, J.; Nagy, A.; Garkusha, I.; Maier, J. P. Higher Energy Electronic Transitions of $HC_{2n+1}H$+ (n=2–7) and $HC_{2n+1}H$ (n=4–7) in Neon Matrices. *J. Chem. Phys.* **2010**, *133*, 024304/1–9.

30) Bieri, G.; Schmelzer, A.; Asbrink, L.; Jonsson, M. Fluorine and the Fluoroderivatives of Acetylene and Diacetylene Studied by 30.4 nm He(II) Photoelectron Spectroscopy. *Chem. Phys.* **1980**, *49*, 213-224.

31) Fulara. J.; Nagy, A.; Filipkowski, K.; Thimmakondu, V. S.; Stanton, J. F.; Maier, J. P. Electronic Transitions of $C_6H_4^+$ Isomers: Neon Matrix and Theoretical Studies. *J. Phys. Chem. A* **2013**, *117*, 13605-13615.

Graphical abstract (TOC):

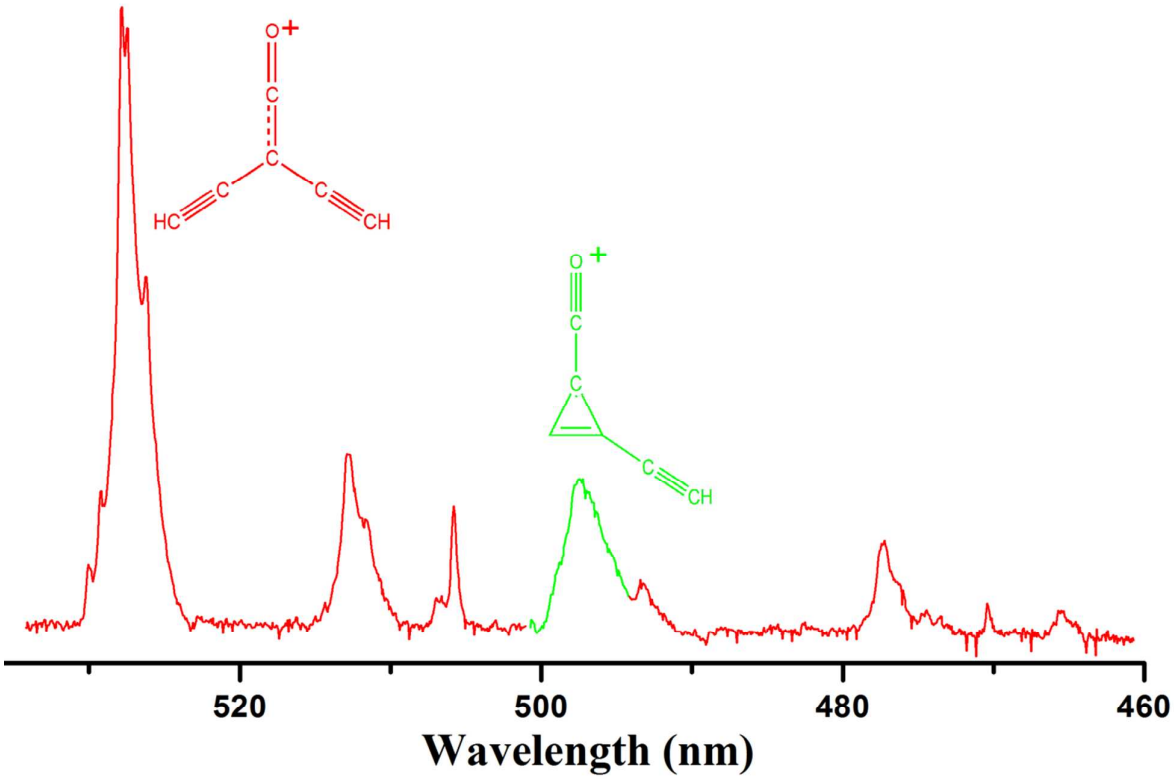

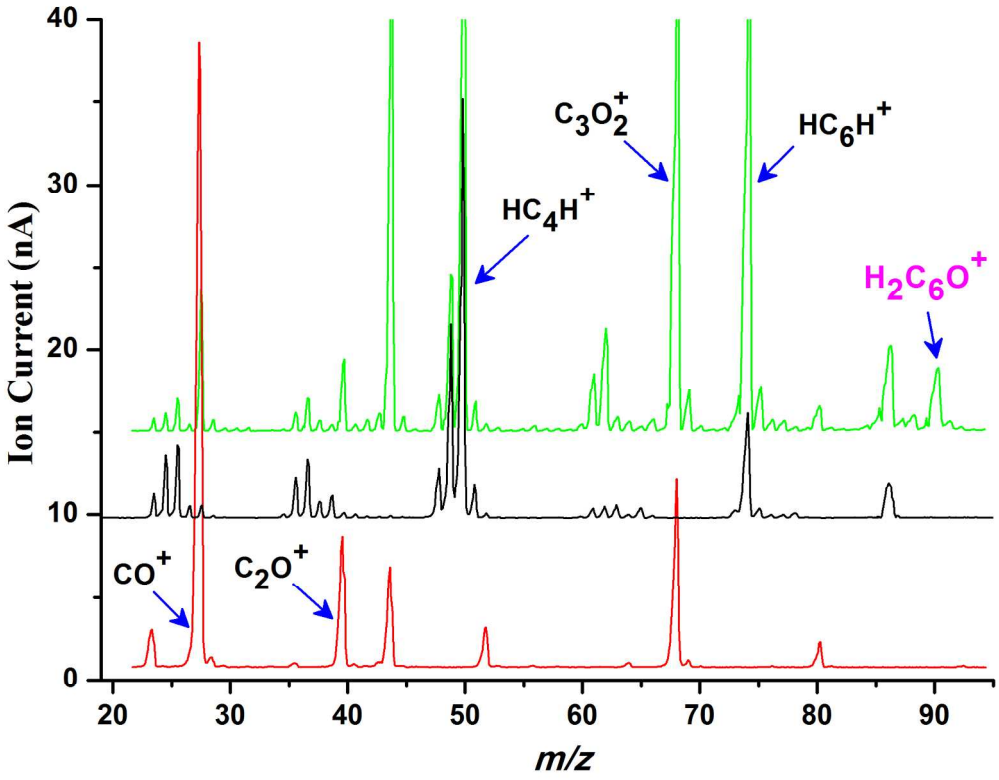

Mass spectra of C3O2 (red), HC4H (black) and 1:1 mixture of C3O2 and HC4H (green). The H2C6O+ (m/z = 90) peak appeared upon mixing C3O2 and HC4H.
179x140mm (300 x 300 DPI)

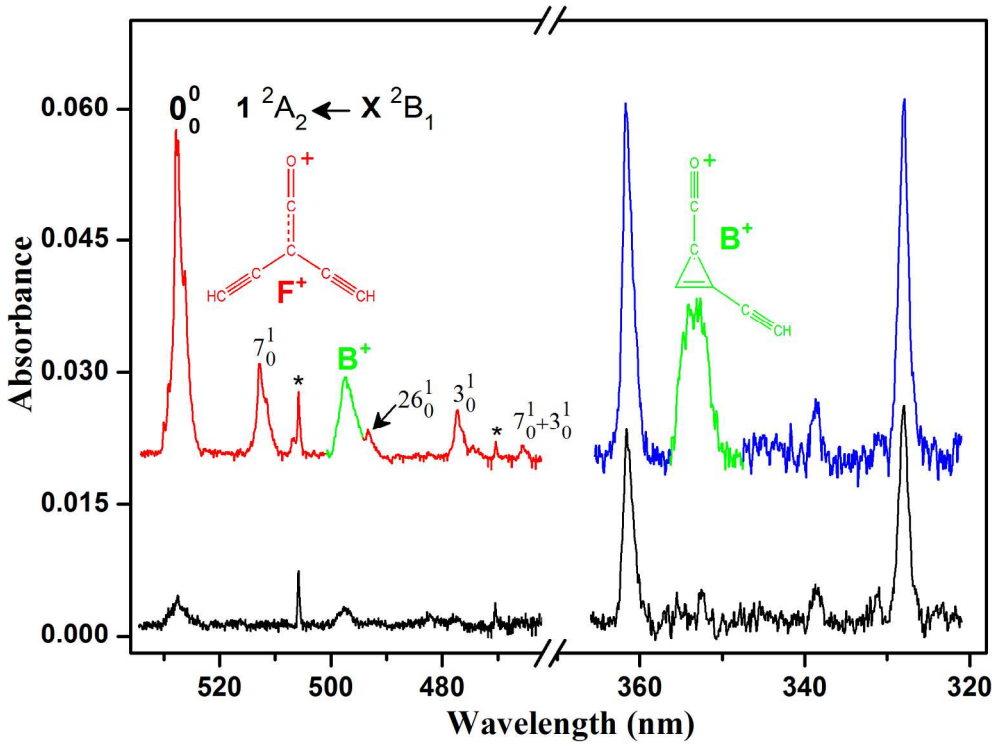

Electronic absorption spectra recorded after deposition of H2C6O+ produced from a 1:1 mixture of C3O2 and diacetylene (upper traces) and after 20 minute irradiation with λ>260 nm photons (lower traces). Bands denoted by * belong to C2+.
179x133mm (300 x 300 DPI)

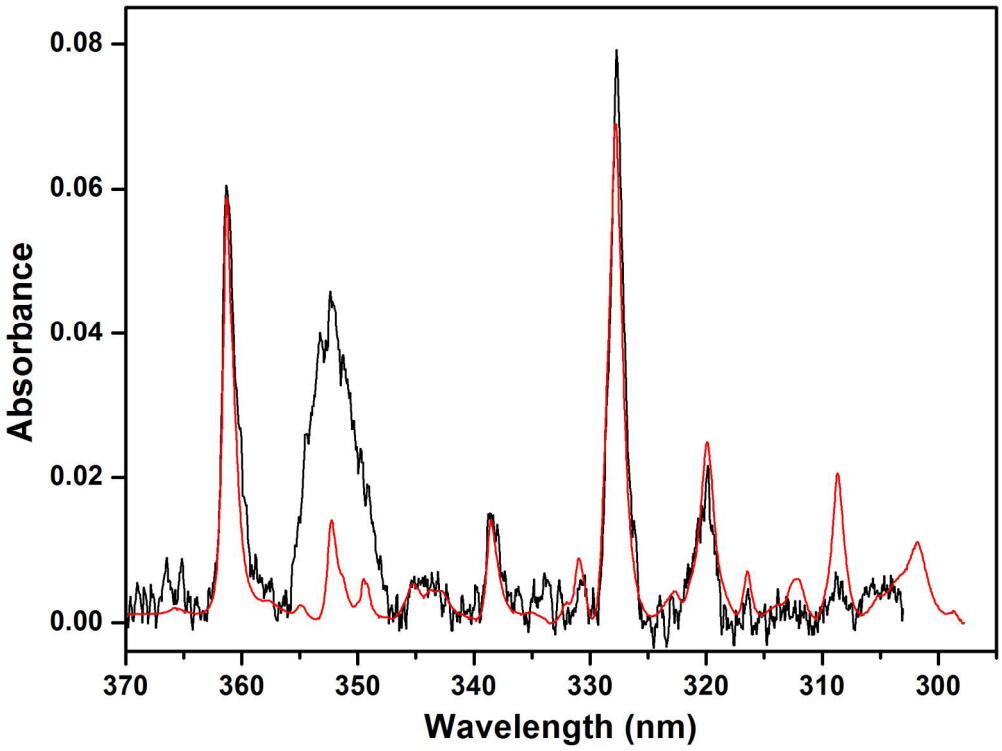

Electronic absorption spectra recorded after deposition of H2C6O+ generated from a 1:1 mixture of C3O2 and diacetylene (black), and after deposition of HC5H+ produced from diacetylene (red). The spectrum of HC5H+ is normalized to the intensity of the 362 nm band.
179x133mm (300 x 300 DPI)

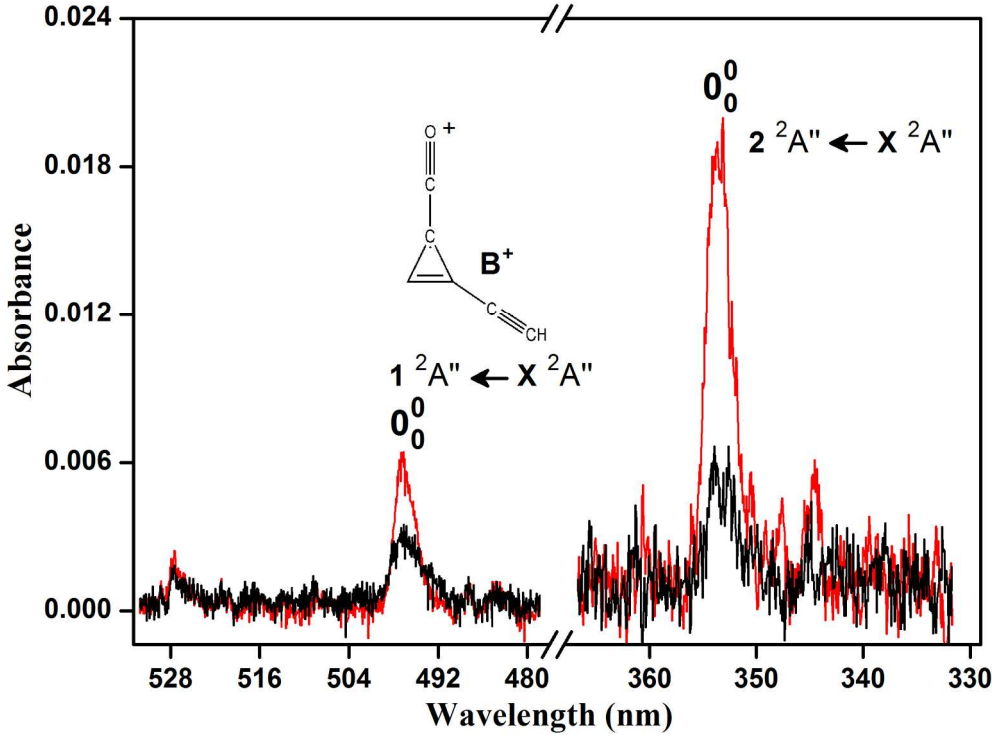

Electronic absorption spectrum of H2C6O+ obtained after deposition of m/z = 90 ions produced from 2, 4, 4, 6-tetrabromo-2,5-cyclohexadienone (TBrC) – red, and after 20 min. irradiation with 250 - 390 nm photons – black.
179x133mm (300 x 300 DPI)

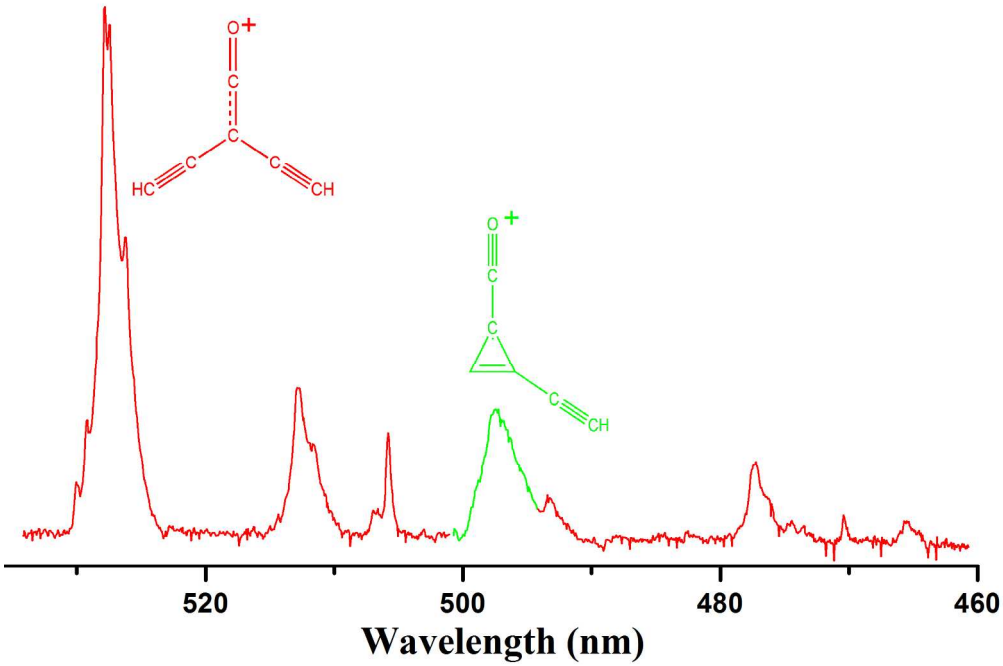

198x139mm (300 x 300 DPI)